

*Proceedings of “Applications of Physics in Mechanical and Material Engineering” (APMME 2023)*

## Numerical Investigation of the Optical Properties Related to Combined Periodic and Porous Surface Structures

M. DOŚPIAŁ\* AND K.M. GRUSZKA

*Department of Physics, Czestochowa University of Technology, Armii Krajowej Ave. 19, 42-200 Czestochowa, Poland*

Doi: [10.12693/APhysPolA.144.346](https://doi.org/10.12693/APhysPolA.144.346)

\*e-mail: [marcin.dospial@pcz.pl](mailto:marcin.dospial@pcz.pl)

In this paper, the results of studies on sub-micrometer planar structures used for aimed frequency-dependent electromagnetic radiation dissipation are presented. The proposed specific geometry of periodic parts of surface structures should enable the occurrence of phenomena related to selective reflectance and interference. The inner porous structure should lead to the formation of destructive interference of electromagnetic radiation and its dissipation. The investigated structures were irradiated by a Gaussian-type radiation source. The propagation was analyzed using the MEEP software package for electromagnetic simulation via the finite-difference time-domain method. The reflectance spectra were obtained by the Fourier transform of the response to the short pulse. The obtained results showed that the surface structures are mainly responsible for reflected electromagnetic spectrum composition, while the porous parts were responsible for thermal radiation dissipation.

topics: finite-difference time-domain (FDTD), electromagnetic (EM) propagation, structural colors, electromagnetic radiation dissipation

### 1. Introduction

In nature, there are many structures, the mapping of which allows the transfer of evolutionarily optimized patterns in order to achieve selected functional properties of chosen technical solutions [1, 2]. Examples of such an approach include the application of structure types met in shark scales in the production of algae-resistant hulls [3], or abalone shells, the structure of which is an inspiration for reinforcement applied in materials engineering [4]. One of such designs is also the wing structure of butterflies from the *Archaeoprepona demophon* family [5] (see Fig. 1), which was the inspiration for the research carried out in this paper.



Fig. 1. Photo of the butterfly of the *Archaeoprepona demophon* family [5].

The biological function of this butterfly wing surface is to obtain angle-dependent reflections, known in science as structural colors, as well as to absorb heat energy from infrared radiation. The introduction of solutions inspired by these phenomena into technical devices may allow for the improvement of heat dissipation technology [6] in devices exposed to high temperatures or the improvement of methods for obtaining colored surfaces that do not lose their properties due to pigment fading [7]. In this paper, we performed a theoretical analysis of the absorption and reflection spectra of structures based on a butterfly wing. For this reason, we have presented the results of FDTD calculations of Gaussian pulse propagation and transmittance spectra evaluated on both porous and periodic surfaces of biologically inspired structures.

### 2. Computational methods

For all calculations, we have used the MEEP software package [8], which implements the finite-difference time-domain (FDTD) method for simulating electromagnetic wave propagation. Based on the areas marked in Fig. 2, the parameters of pores present in the substrate structure were determined. It was found that their moderate size was about  $0.4 \mu\text{m}$ . Figure 3 was used to determine the structural parameters of the periodic pattern present in a wing surface [9]. The analyzed transmission electron microscopy (TEM) images

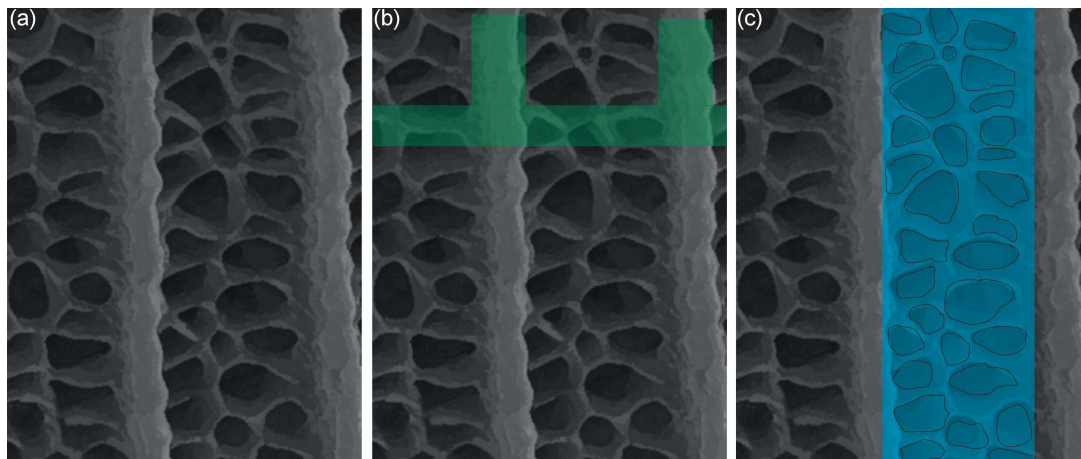


Fig. 2. TEM images of butterfly wing with marked characteristic patterns that were transferred to theoretical model [9].

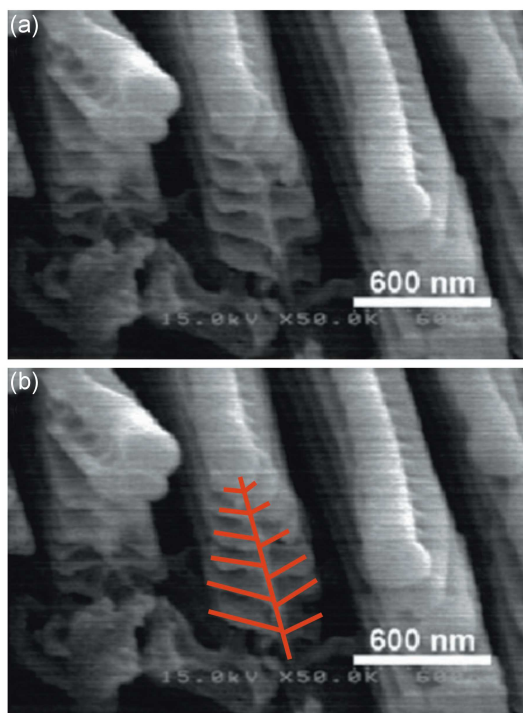


Fig. 3. TEM images of butterfly wing with cross-section pattern with marked characteristic structures that were transferred to theoretical model [9].

revealed that the observed structures have tree-like patterns. The height of observed trees was moderately  $1.5 \mu\text{m}$ . The branches on that pattern had about  $0.05 \mu\text{m}$  thickness and the same distance between themselves. Their length decreased with the distance from the base of the trunk from  $0.4$  to  $0.05 \mu\text{m}$ . The distances between neighboring patterns were around  $0.05 \mu\text{m}$  on the bottom of the structure.

The obtained parameters allowed us to create 6 basic shapes of different complexity. All analyzed shapes are presented in Fig. 4a-f.

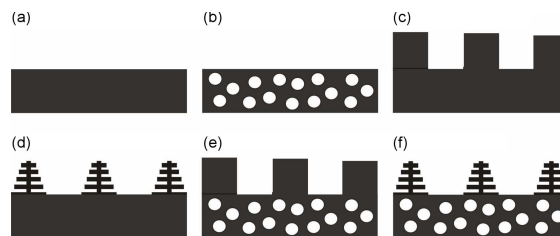


Fig. 4. Types of structures analyzed in the model: (a) reference structure of substrate, (b) substrate with holes, (c) substrate with a surface ridge (comb structure), (d) substrate with surface Christmas tree pattern, (e) substrate with holes and surface ridge, (f) substrate with holes and Christmas tree pattern.

A substrate in the form of a simple block was used as a basic reference structure, as presented in Fig. 4a. Then, the porous substrate, as well as substrates with surface periodic patterns, were chosen for further analysis (see Fig. 4b–d). The last part of the analysis was performed for combined structures, as presented in Fig. 4e, f. The optical property, i.e.,  $\epsilon$  value, was set to 2.44 for all solid structures, which is similar to values found in the literature [9]. The light source was placed in front of the structure, in the middle, at a distance of  $6 \mu\text{m}$ . In applied simulation, space was set as a 2D  $16 \times 16 \mu\text{m}^2$  and was digitized. The 60 pixels represented a length of  $1 \mu\text{m}$ . Also, in order to reach numerical stability, a 0.5 Courant criterion was used. Based on such assumed variables and the working area, the time step in the simulation was 5 ns. The Gaussian pulse was set in TE mode (TE — electric part of the electromagnetic wave) in such a way that in 2D simulation the  $E_x$  and  $E_y$  components of the electromagnetic field were parallel to the  $x$  and  $y$  axis of the computational domain, respectively. The component  $E_z$  was the current component, which was modulated in time. Due to the

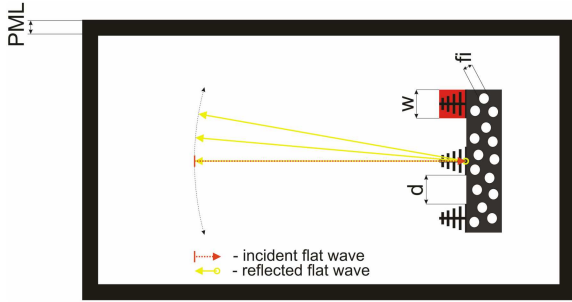


Fig. 5. Scheme of the measurement environment implemented in the MEEP program to perform theoretical research.

MEEP program using current types of sources, the source used in the simulation was not a hard type. Such prepared structures and the light source were placed in the air area surrounded by PMLs (perfectly matched layers) of  $1 \mu\text{m}$  thickness, as can be seen in Fig. 5.

The transmittance spectra were obtained by the Fourier transform of the response to a short pulse of a flat wave. The Fourier transform was calculated just after an analyzed structure, before PML. The calculations were performed along a vector perpendicular to the longer side of the substrate. The obtained transmittance results were normalized by a similar calculation performed for a source placed in an empty box filled with air. Gaussian-pulse radiation source, with  $1.875 [2\pi C/a]$  central frequency and  $3.223 [2\pi C/a]$  width, which represents UV(A)–VIS–IR(A) wavelength area, was used for both types of calculations.

### 3. Results and discussion

In Fig. 6, the electromagnetic (EM) wave propagation in the computational cluster with different types of reflecting/absorbing structures was presented. Red and blue colors on the exposed picture represent positive and negative peaks of  $E_z$  component of the electromagnetic field with respect to the surroundings in white, which are treated as zero amplitude. The EM source applied in the simulation generated flat pulses that have a temporal intensity profile, which has a Gaussian shape. Subjecting such an impulse to a Fourier analysis reveals that in its spectrum, different frequencies appear, distributed around the  $1.875 [2\pi C/a]$  central frequency, with a width of distribution equal to  $3.223 [2\pi C/a]$ . In all the panels of Fig. 6, three different areas of EM distribution can be seen. The first area represents the emitted pulse modified by its backward superposition with a reflected wave from the surface of a structure. The second one represents internal propagation in the substrate region. The last area represents the transmittance region behind the structure. As can be seen in Fig. 6a, b, d, e, the

EM pulse for any periodic structure results in the presence of a reflected flat return pulse in the backward direction, but also a clearly visible symmetrical bent at an accurate angle for the Christmas tree-shaped structure and at a wide angle of deflection for the comb structure. For a substrate without a periodic structure, we only observe distinctive back reflection. In the second area, the inner zone of the substrate, the pulse propagation frequency is changed. It increases the most for solid areas without a periodic structure or with a structure in the form of a comb; for the substrate behind the Christmas tree structure, the observed changes in the propagation frequency are weaker. In porous areas, they remain unchanged in relation to the incident pulse. EM propagation for the last area in the transmittance region behind the examined structure was focused and significant for the comb surface pattern, dissipated but clearly present for the Christmas tree surface pattern, and almost vanished for the plane surface and porous structure. The presence of combined structures resulted in moderate transmittance compared to less complex structures (lower than for surface patterns with a solid substrate and smaller than for those with a plain porous substrate).

In Fig. 7, the transmission, reflectance, and summarized loss spectra for all investigated structures are presented. As can be seen in Fig. 7a, the substrate made of a flat block has the smoothest shape of all dependencies for VIS–IR(A) wavelengths. In the UV(A) region, sharp peaks on transmission and reflectance curves are present. This type of structure strongly reflects selective values of UV(A) and the whole VIS area, especially wavelengths from the blue VIS region. Reflectance rapidly decreases in the IR(A) area. Transmittance spectra in the reference structure show reversed behavior to reflectance spectra, i.e., high values for selective wavelengths in the UV(A) region and rapid growth in the red VIS–IR(A) wavelength area. Losses observed for that structure have very low values for short waves, starting from about a few percent and increasing systematically to approximately 20% for a wavelength of 700 nm. The introduction of periodic structures (Fig. 7b and d) on the surface of the analyzed sample leads to the creation of irregular, jagged dependence for all measured quantities. The analysis of the loss dependence shows that for both tested structures, there is a clear increase in their overall value. For the comb-shaped surface structure, the greatest changes occur within UV(A) and VIS regions up to a value of approximately 600 nm. Their value reaches an average of 50% and a maximum of 75% for the 450 nm peak. For wavelengths above 600 nm, they assume an average value of 20%. All these changes mainly correspond with a reduction of reflectance, with the exception of the UV(A) region, where changes correspond to a reduction in both transmittance and reflectance quantities. Analysing Fig. 7c, it can be seen that the presence of holes in the substrate leads to



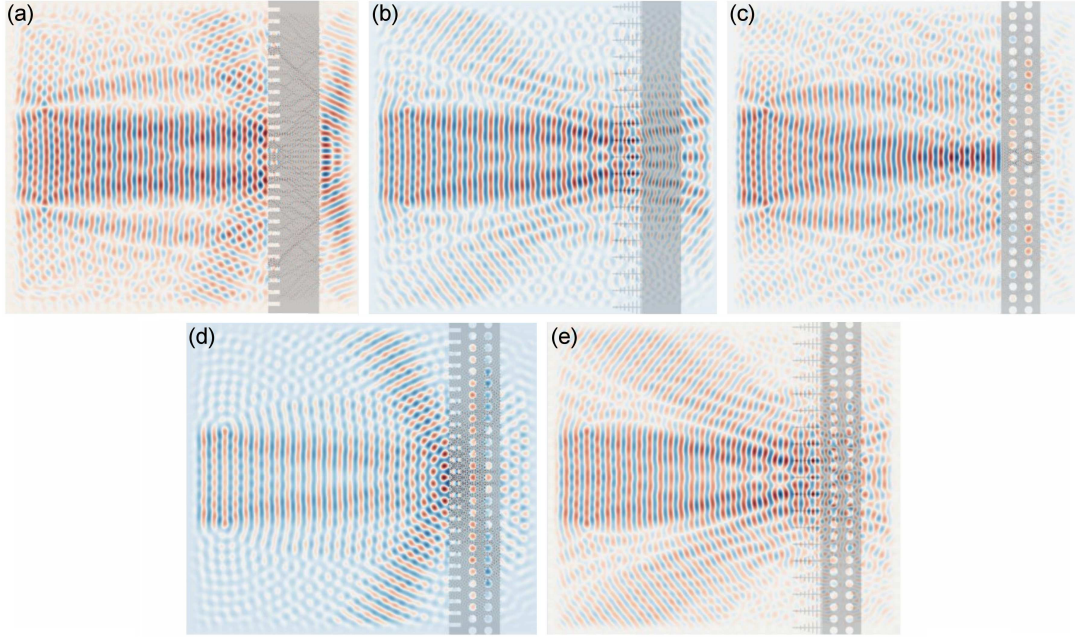


Fig. 6. EM wave propagation in the computational cluster, with five types of reflecting structures: (a) substrate with holes, (b) substrate with surface ridge (comb structure), (c) substrate with surface Christmas tree pattern, (d) substrate with holes and surface ridge, (e) substrate with holes and Christmas tree pattern.

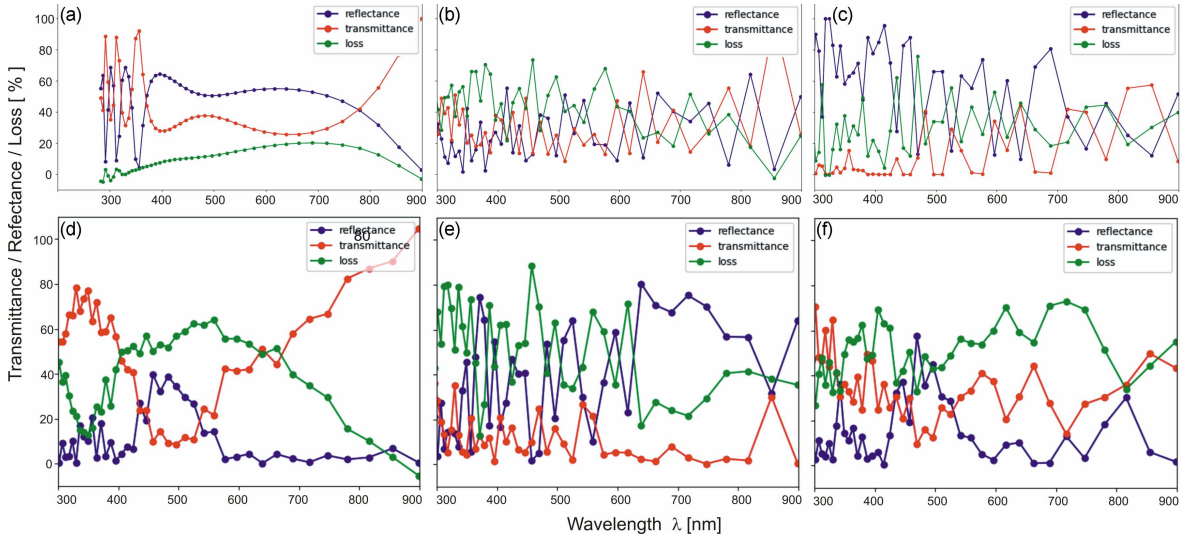


Fig. 7. Transmission spectra for EM wave propagated in the computational cluster, with five types of reflecting structures: (a) reference block substrate, (b) block substrate with surface ridge (comb structure), (c) block substrate with holes, (d) block substrate with surface Christmas tree pattern, (e) block substrate with holes and surface ridge, (f) block substrate with holes and Christmas tree pattern.

vanishing transmittance almost on the whole spectrum, with exceptions seen for chosen frequency peaks of intensities lower than 50%. We also note a large increase in reflected rays in the short wave region, which is slowly fading till 700 nm wavelength. Over that value, reflectance varies around 50%. The losses generally increased to moderately 35%, achieving the highest value of 75% for a peak near 475 nm. Interesting results were also obtained

for tree-like surface structure in Fig. 7d. All dependencies had a less jagged structure than that observed for the rest of the modified samples. It was observed that the maximum of losses shifted from the red-VIS region in the direction of shorter wavelengths, compared to the reference structure. Its middle was found at 550 nm and had a 3.5 times higher value. The changes observed in the transmittance spectrum were also significant. The presence

of a wide optic window for UV(A) was found. Over that window, transmittance fell down to almost 10%, and starting from 550 nm, grew systematically to reach 100% near 900 nm. From an analysis of reflectance spectra in Fig. 7d, one can see that almost in all examined regions, reflectance was close to 0% except in the area of wavelengths from 400 to 550 nm. That shows the presence of reflection in the blue–green VIS region. The combination of surface structure and holes in the substrate leads to different effects. In the case of a comb structure with holes on the substrate, we can see the growth of losses, especially for shorter waves, and an increase in reflectance for longer wave area (over 600 nm). Transmittance fades almost to 0% except in some narrow areas, especially for short waves in the UV(A) region. In the case of a tree-like surface structure with pores in the substrate, we can see that the strongest reflection is still present in the blue–green VIS region, but there are also small amounts of rays reflected in the IR(A) region from 750 to 850 nm. The losses are quite high, but transmittance is higher than for the sample with the same surface structure and lack of holes.

#### 4. Conclusions

In this paper, a theoretical analysis of the absorption and reflection spectra of structures based on a butterfly wing was performed.

The results of FDTD calculations of Gaussian pulse propagation and transmittance spectra evaluated on biologically inspired structures revealed that the porous structure of the substrate was responsible for a dissipation of the electromagnetic radiation. This observation is based on the increase in recorded losses as well as reflected radiation. The obtained results are coherent with postulated assumptions.

The periodic comb-like structure led to a more jagged dependence of all quantities, while another periodic structure, a tree-like one, was responsible for the increase in losses as well as transmittance in UV(A), VIS-red, and IR(A) areas. In this case, the reflectance was reduced to blue and green VIS

region. The reflectance in such a range is coherent with the structural colors of the investigated biological structure and is a proof that the structure parameters for the tree-like surface model have been selected correctly.

To sum up, the use of structures based on pores leads to the dissipation of EM radiation, and the Christmas tree structure allows to obtain structural colors.

#### Acknowledgments

This research was supported in part by PLGrid Infrastructure.

#### References

- [1] H. Xue, D. Liu, D. Chi, C. Xu, S. Niu, Z. Han, L. Ren, *Adv. Mater. Interfaces* **8**, 2100142 (2021).
- [2] M. Dośpiał, K.M. Gruszka, *Acta Phys. Pol. A* **142**, 35 (2022).
- [3] X. Pu, G. Li, H. Huang, *Bio. Open* **5**, 389 (2016).
- [4] Y.-Y. Sun, Z.-W. Yu, Z.-G. Wang, *Adv. Civil Eng.* **2016**, 1 (2016).
- [5] *Nymphalidae*, *Wikipedia*, 15.11.2023 (in Polish).
- [6] Y. Cui, D. Li, H. Bai, *Ind. Eng. Chem. Res.* **56**, 4887 (2017).
- [7] F. Chen, Y. Huang, R. Li, S. Zhang, B. Wang, W. Zhang, X. Wu, Q. Jiang, F. Wang, R. Zhang, *Chem. Commun.* **57**, 13448 (2021).
- [8] A.F. Oskooi, D. Roundy, M. Ibanescu, P. Bermel, J.D. Joannopoulos, S.G. Johnson, *Compu. Phys. Commun.* **181**, 687 (2010).
- [9] G. Zyla, A. Kovalev, M. Grafen, E.L. Gurevich, C. Esen, A. Ostendorf, S. Gorb, *Sci. Rep.* **7**, 17622 (2017).